Radiopaque Acrylic Bone Cements with Bromine-Containing Monomer

Marius Ciprian Rusu,[1] Constanta Ibanescu,[1] Ionut Cameliu Ichim,[1] Gerard Riess,[2] Marcel Popa,[1] Daniela Rusu,[3] Mihai Rusu[1]

[1]*Chemical Engineering Faculty, "Gh. Asachi" Technical University, 700050, Iasi, Romania*
[2]*Laboratoire de Chimie Macromoléculaire—ENSCMu, 68093, Mulhouse Cedex, France*
[3]*CEMEF, Ecole de Mines de Paris—ParisTech, Sophia-Antipolis Cedex, France*

Received 7 January 2008; accepted 30 July 2008
DOI 10.1002/app.29253
Published online 25 November 2008 in Wiley InterScience (www.interscience.wiley.com).

ABSTRACT: One important issue for the acrylic bone cements concerns the radiopacity, which may be achieved by different ways. In this work, a new bromine-containing acrylic monomer, the 2-(2-bromopropionyloxy) propyl methacrylate (BPPM), was synthesized and proposed to be used for providing radiopaque bone cements. Different acrylic bone cements were realized by partially replacing the methyl methacrylate (MMA) monomer phase with 5–20% w/w of BPPM-comonomer. The effect of this comonomer on the curing parameters of acrylic bone cements, on their thermal and rheological properties, water absorption, density, contact angle, compression tests, and radiopacity was studied. It appears that the presence of BPPM does provide radiopacity, improves the curing parameters by decreasing the maximum curing temperature and increasing the setting time. The new BPPM-acrylic bone cements exhibit lower glass transition temperature and better thermal stability when compared with the classical radiolucent acrylic cements. Rheological measurements have shown that 10–20% w/w of BPPM in the liquid phase of acrylic bone cement formulations increase its flexibility, and may also induce a slight crosslinking reaction during the curing phase. BPPM-modified acrylic bone cements present lower polymerization shrinkage and higher compression strength, and similar water uptake, porosity, and water contact angle as the radiolucent PMMA-cements. © 2008 Wiley Periodicals, Inc. J Appl Polym Sci 111: 2493–2506, 2009

Key words: biomaterials; acrylic bone cements; bromine-containing acrylic monomer; rheology; radiopacity

INTRODUCTION

Acrylic bone cements are extensively used in orthopedics for fixing prosthetic devices to bones.[1–3] In these applications, the main function of the cement is to serve as interfacial phase between the prosthesis and bone, thereby assisting to transfer and distribute loads in the "prosthesis-bone cement-bone" system.[1,4]

Commercial acrylic bone cements are usually based on poly(methyl methacrylate) (PMMA). They consist of a solid polymer phase (mainly PMMA beads or related copolymer) and a liquid monomer phase (methyl methacrylate, MMA). After mixing the two phases, the polymerization takes place via free radical reaction of the monomer. The polymerization kinetics is not only controlled by the monomer-to-polymer ratio, but also by the concentrations of the initiator (e.g., benzoyl peroxide), present in the solid phase and the activator (e.g., *N,N*-dimethyl-*p*-toluidine), present in the liquid phase.[1–3] As the polymerization reaction proceeds in situ, the powder/liquid mixture progresses from viscous liquid to dough consistency and finally a rigid, amorphous polymer, within 10–15 min.[5,6]

Orthopaedic acrylic bone cement have to fulfill several medical requirements, such as moderate setting times (so that the cement does not cure too fast or too slowly), low values of maximum curing temperature (to avoid thermal necrosis of the bone tissue, during the setting of the cement), high values of compressive strength (allowing the cured cement mantle to withstand the compressive loads involved by normal daily activities). It is also essential for the acrylic bone cements to be radiopaque, to allow radiological detection.[7,8] However, the radiopacity of orthopedic acrylic bone cement itself is very limited, because of the low density of the polymeric materials (macromolecular structures containing light elements such as hydrogen, oxygen, and carbon). Radiopacity has been frequently achieved by adding X-ray contrast materials, such as barium sulfate or zirconium dioxide, which are also known to alter the biological and mechanical properties of the bone cement.[2,5,7–11]

Considering all these aspects, some alternatives to the traditional inorganic radiopacifying agents have

Correspondence to: M. C. Rusu (mrusu@ch.tuiasi.ro).
Contract grant sponsor: Romanian Ministry of Education and Research.

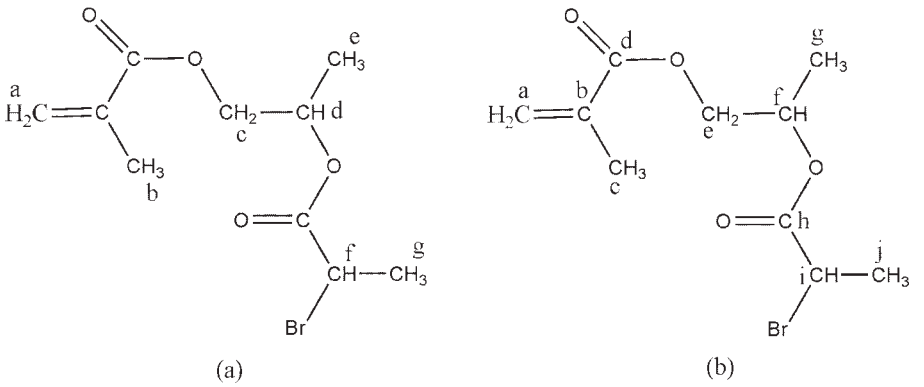

Scheme 1 Chemical structure of BPPM with noted protons for ^{1}H NMR (a) and ^{13}C NMR (b) spectra analysis.

been put forward.[8,12–16] One approach consists in introducing radiopaque-monomeric units during the polymer synthesis. Monomers having covalent-bounded halogen atoms such as iodine and bromine, possessing radiopaque properties, can be copolymerized with classical monomers (such as MMA), to form the final bone cement. In this line, some iodine-containing methacrylates have been proposed for different clinical applications.[13,16,17] More specifically, in the field of the acrylic bone cement, the possibility to confer radiopacity by introducing iodine-containing methacrylates in the liquid monomer phase has been studied.[7,8,15–17]

Although it is well-known that some bromine-containing organic compounds may be used as contrast agents,[18] there are no information regarding their use to confer radiopacity to acrylic bone cements. Our research proved relatively simple acrylic bromine-containing monomers may provide radiopaque bone cements.

This article deals with modification of acrylic bone cement formulations by introducing a bromine-containing monomer in the liquid monomer phase, the 2-(2-bromopropionyloxy) propyl methacrylate (BPPM), which was synthesized in the laboratory.[18]

MATERIALS AND METHODS

Materials

MMA (Aldrich), 2-hydroxypropyl methacrylate (Aldrich), 2-bromopropionic acid (Acros Organics), thionyl chloride (Acros Organics), tetrahydrofuran (Acros Organics), pyridine (Aldrich), *p*-xylene (Fluka), *N*,*N*-dimethyl-*p*-toluidine (DMPT) (Aldrich), and benzoyl peroxide (BPO) (Aldrich) were used as received. The 2-(2-bromopropionyloxy) propyl methacrylate was synthesized in the laboratory. PMMA beads (medical grade) were supplied by Astar SA (Cluj-Napoca, Romania).

Synthesis of 2-(2-bromopropionyloxy) propyl methacrylate

The synthesis comprised two steps.[18] First, 2-bromopropionyl chloride was synthesized by the reaction between 2-bromopropionic acid and thionyl chloride. Second, the 2-(2-bromopropionyloxy) propyl methacrylate was synthesized by the reaction between 2-hydroxy-propyl methacrylate and 2-bromopropionyl chloride, using tetrahydrofuran as solvent and pyridine as HCl acceptor.

After purification, the product structure was identified via ^{1}H NMR and ^{13}C NMR (Scheme 1): ^{1}H NMR (400 MHz) $CDCl_3$, δ (ppm): 6.04 (a); 5.52 (a); 5.17 (f); 4.29 (c); 4.13 (d); 1.87 (b); 1.73 (e); 1.24 (g). ^{13}C-NMR (100.6 MHz) $CDCl_3$, δ (ppm): 169.44 (h); 166.74 (d); 135.68 (b); 126.07 (a); 69.77 (e); 65.81 (f); 39.86 (i); 21.34 (j); 18.13 (c); 16.07 (g).

Methods

Preparation of acrylic bone cements

The new experimental BPPM-bone cements have as starting point a standard formulation for radiolucent acrylic bone cements obtained by adding the MMA liquid phase to the solid phase (PMMA), at room temperature (23°C), in a typical solid/liquid ratio of 2 : 1. For the new formulations, different amounts of MMA (the base monomer) have been partially replaced with the new (co)monomer, BPPM. Four experimental acrylic bone cements have been prepared: with 5, 10, 15 or 20% w/w BPPM in the liquid phase (Table I). All formulations contain 1.5% w/w DMPT (activator) in the liquid phase and 2% w/w BPO (polymerization initiator) in the solid phase (Scheme 2).

Preparation of the acrylic bone cements was carried out following the usual procedure for acrylic bone cements, as described in the ASTM Standard.[6] Both phases (powder and liquid) and all the other devices used in the experiment were allowed to equilibrate at room temperature for 2 h prior to

TABLE I
Composition of the Liquid and Final Phases for the BPPM-Acrylic Bone Cement Formulations

Formulations	Monomer ratio		BPPM content in the feed composition (% w)
	MMA	BPPM	
BPPM-0	100	–	–
BPPM-5	95	5	1.66
BPPM-10	90	10	3.33
BPPM-15	85	15	5.00
BPPM-20	80	20	6.66

mixing. Next, the components of the acrylic bone cements were hand-mixed in a ceramic bowl with a ceramic spatula, at about 1 Hz. When the dough state was reached, the cement mass was placed into the corresponding mold and allowed to cure for 1 h.

Characterization

The acrylic bone cement formulations were systematically characterized by measuring the curing parameters, thermal, and rheological characteristics, water absorption and water contact angle, density, compression tests, and radiopacity.

The curing parameters were recorded at 23°C, according to the ASTM Standard.[6] The time and temperatures were measured from the onset of the mixing powder with the liquid phase. Two determinations were performed for each acrylic bone cement formulation.

The thermal properties were determined by differential scanning calorimetry (DSC) and thermogravimetric analysis (TGA). The DSC was performed on a Pyris Diamond DSC (Perkin–Elmer, USA). The samples, obtained by cryogenic grinding of the cured cements, in powder form (8–12 mg), were introduced in aluminum pans and then heated from 10 to 160°C, at a constant rate of 20°C/min. Glass transition temperatures (T_g) were determined on the second scan, considering the onset of transition. The TGA was carried out under nitrogen flow (25 cm^3/min), at a heating rate of 15°C/min, from 25 to 700°C using a Mettler Toledo TGA/SDTA 851 (Mettler-Toledo AG, Switzerland). The initial weight of the samples was around 4.5–7.5 mg.

The rheological measurements were performed on a Physica MCR 501 rheometer (Anton Paar, Austria)

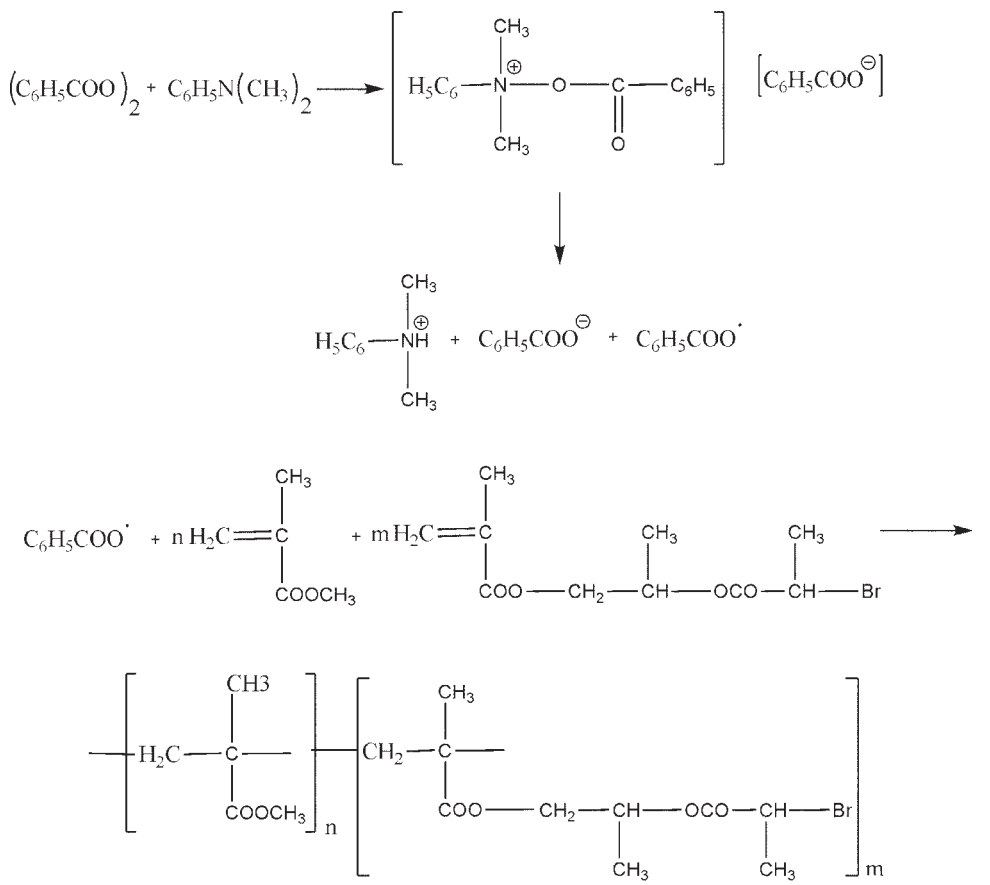

Scheme 2 Copolymerization reaction scheme of MMA and BPPM.

equipped with electronically commutated synchronous motor, allowing rheological measurements in controlled-stress and controlled-strain modes.[19] The polymer samples were heated using a Convection Temperature Device CTD 600, with direct detection of the sample temperature. All measurements where carried out in a parallel-plate geometry with a diameter of 25 mm, and a gap of 1 mm. Sample degradation was prevented by working under nitrogen atmosphere.

The water absorption of the acrylic bone cement formulations was studied by immersing dry disk samples (3.5 mm thickness, 10 mm diameter) in 100 mL of distilled water, at 23°C. The samples were weighed at different times until the equilibrium hydration degree was attained.

The apparent densities of acrylic bone cement formulations were determined by picnometer method,[20] using ethanol as immersion liquid. The maximum densities were calculated according to a method presented in literature.[21] The polymerization shrinkage and porosity are directly related to density.

Water contact angle measurements were performed on cement samples, at room temperature, using a contact angle measuring system Kruss K 121 (Kruss GmbH, Hamburg) with software for fully automatic contact angle determination.[22]

Compressive tests were carried out on cylindrical specimens (6 mm diameter and 10 mm high), on a mechanical testing machine (Tyratest, Germany), using a load of 100 kN and a cross-head speed of 5 mm/min, at room temperature. Tests were conducted up to failure or until 70 or 80% reduction in specimen height. Five specimens were tested for each formulation and their compressive strength (C_S) was calculated as $C_S = F/A$, where F is the application load and A is the area of the test specimen.

The radiographic study was carried out on a standard General Electric X-ray instrument (set at 55 kV and 2.5 MAS). The relative X-ray opacity was visually determined.

RESULTS AND DISCUSSION

Curing parameters

The free radical polymerization of monomers forming the liquid phase of acrylic bone cement formulations is an exothermic reaction, and the generated heat increases the system temperature during cement curing (Fig. 1). This exothermy varies according to the chemical composition of monomer liquid phase (i.e., 544 J/g for MMA), the powder/liquid ratio, and the nature of the radiopaque agent.[23–27]

With regard to the orthopedic application, the main curing parameters such as peak temperature

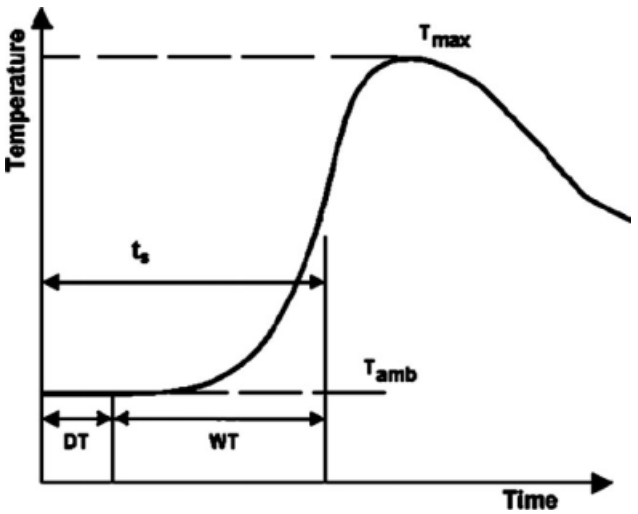

Figure 1 Change in polymerization temperature versus time (T_{max}, maximum curing temperature; T_{amb}, room temperature; DT, doughing time; WT, working time; t_s, setting time (the time when bone cement temperature reaches the half of the difference between T_{max} and T_{amb}, $\frac{T_{max}-T_{amb}}{2}$, according to the ASTM Standard[6]), $T_{ts} = T_{amb} + \frac{T_{max}-T_{amb}}{2}$).

(maximum temperature, T_{max}), temperature corresponding to setting time (T_{ts}), setting time (t_s) and working time (implicitly, the time of reaching maximum temperature, t_{Tmax}) are crucial for cement handling and the success of the surgical procedure. The peak temperature is considered to be the maximum temperature reached during the polymerization reaction, and the setting time can be determined according to the ASTM standard as follows[6]:

$$T_{amb} + (T_{max} - T_{amb})/2 \quad (1)$$

where T_{max} is the maximum temperature in °C and T_{amb} is the ambient temperature (23°C).

Figure 2 and Table II present the temperature profiles and the curing parameters (T_{max}, t_{Tmax}, t_s, T_{ts}) corresponding to the cement formulations from Table I.

As can be seen, all formulated acrylic bone cements exhibited T_{max} much lower than the value established by the ASTM Standard (90°C).[6] Furthermore, T_{max} significantly decreases when adding the bromine-containing monomer, and with increasing the BPPM content in the cement formulation. This means that the new BPPM-acrylic bone cement formulations are supposed to cause less adverse effects on the surrounding bone tissues, at least as far as concerning the curing temperature.[8,28–32] The T_{max} values obtained for acrylic bone cements modified with bromine-containing comonomer are similar with the values presented in literature for acrylic

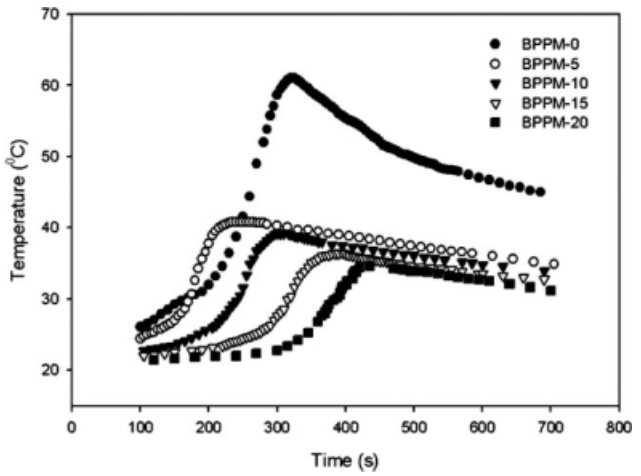

Figure 2 Polymerization exotherms for the BPPM-acrylic bone cement formulations.

bone cements modified with iodine-containing comonomers.[7,8,15–17]

They are two reasons for this effect of the BPPM content on the maximum curing: first, the exothermic effect depends on the number of acrylic groups susceptible to react during the polymerization process, and replacing 5–20% w of MMA with BPPM (acrylic monomer with the molecular weight 2.66 times larger than the one of MMA) will diminish the number of moles of acrylic monomers in the system. Consequently, the amount of generated heat per mass unit will decrease. In addition, the lower and slow release of the polymerization heat during the curing reaction allows gradual heat dissipation through the mass, leading to a lower T_{max}.

The setting temperature is strongly related to T_{max}, and its value decreases as well with increasing the BPPM content in the cement formulations. The corresponding setting time and the time of reaching T_{max} are comparable or even higher than the ones for the radiolucent cement, as soon as the added BPPM content in the initial liquid phase exceeds 10% w/w. This behavior is a result of a reduced reaction rate in liquid phase, because of a lower number of double bonds on mass unit in monomer mixture as compared with only MMA and selective absorbtion of comonomers in PMMA solid phase. Similar results have been reported when part of MMA was replaced with iodine-containing monomers [8,15–17]. This represents a second significant advantage with respect to the orthopedic application, because the new BPPM-bone cement formulations allow longer but not excessive working time as comparing with the classical PMMA-cements.[8,29] Preliminary tests showed that new formulated acrylic bone cements modified with BPPM comonomer present a good biocompatibility. A study about the toxicity of bromine-containing monomer is in progress.

Thermal properties

The influence of BPPM-modified cement formulations on glass-transition temperature (T_g), and the heating behavior of the new acrylic bone cements were determined. The T_g of the acrylic bone cements is an important parameter, as it may be related to the flexibility and toughness of these cured biomaterials. Generally it is assumed that materials with high T_g are brittle, which is indirectly related to the failure of the cement and, subsequently, to components loosening.[31]

Figure 3 and Table III show the influence of BPPM-content in the cement formulation on the T_g and sample thermal stability (Fig. 4), with regard to heating temperature (TGA) and sample decomposition (DTG). As can be seen, replacing 10–20% w/w of MMA from the cement liquid phase with our bromine-containing monomer induces a notable decrease of the T_g. This decrease may be correlated with the higher mobility of the system-born chain segments of the copolymer (BPPM-*co*-MMA) because of the large lateral substituents of BPPM. When BPPM content increases from 10 to 20% w/w, a small decrease for the T_g of the BPPM-acrylic bone cements is noticed, meaning that BPPM-10 and BPPM-20 exhibit better flexibility than the radiolucent PMMA-formulation.

The similar shapes of TG and DTG-diagrams for BPPM-0, BPPM-10, and BPPM-20 indicate that the new comonomer does not modify significantly the heating behavior of the acrylic bone cements. However, the onset temperature (T_{onset}) of the thermal decomposition of BPPM-acrylic bone cements is 40–70% higher than the one for radiolucent cement, indicating a better thermal stability of the BPPM-modified cements as comparing with PMMA-cements.

Rheological properties

Most of the research on acrylic bone cements fixed prostheses was devoted to static analysis.[33–35] Very

TABLE II
Curing Parameters for the BPPM-Acrylic Bone Cement Formulations

Formulation	T_{max} (°C)	t_{Tmax} (s)	t_s (s)	T_{ts} (°C)
BPPM-0	61.0	320	250	41.0
BPPM-5	40.8	240	175	30.9
BPPM-10	39.2	300	245	30.1
BPPM-15	36.4	390	310	28.7
BPPM-20	34.5	440	370	27.7

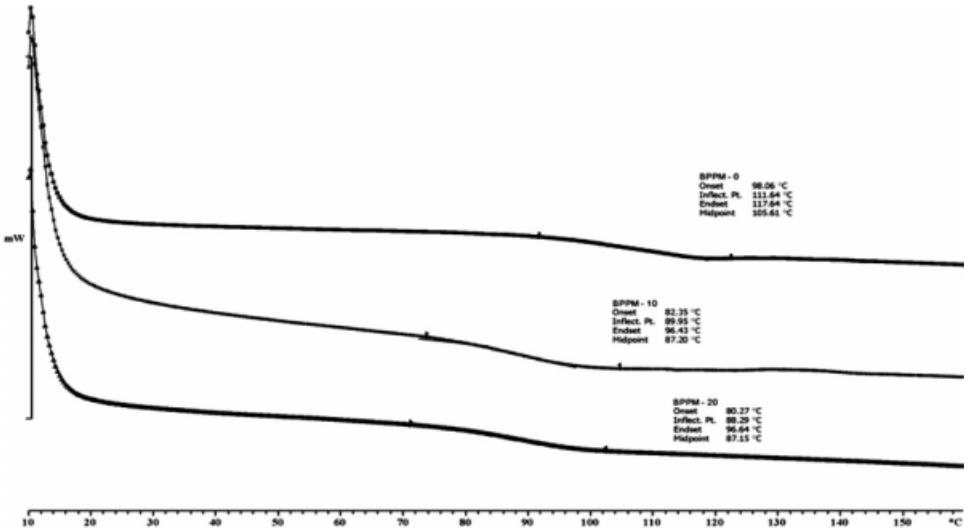

Figure 3 DSC curves for BPPM-0 (■), BPPM-10 (x), BPPM-20 (▲).

few researches focus on dynamic analysis of prostheses.[35,36] However, the elements design for static loading could fail under dynamic loading conditions such as walking, since the dynamic add up to about 10–20% or more loading to the prosthesis. This fact has to be taken into account to avoid fracture or failure of the prosthesis.[37] The acrylic bone cements used to fixing prosthetic devices is assisting to transfer/distribute loading in the "prosthesis-bone cement-bone" system, and thus it is concerned as well by cyclic loadings.

This rheological study is also intended to provide useful information on the new BPPM-acrylic bone cements from structural viewpoint and by comparison with the PMMA-radiolucent formulation.

Viscoelastic effects of the materials can be efficiently evaluated via oscillatory measurements as both components of the viscoelastic behavior are represented by the storage modulus G' (elastic part) and the loss modulus G'' (viscous part). The storage modulus G' gives information about the elastic character of the material, or the energy stored during the deformation. The loss modulus G'' tells about the viscous character of the material, or the energy dissipation that occurs in flow.

Oscillatory tests allow the investigation of a large range of viscoelastic materials, from low-viscosity liquids to polymer solutions and melts, pastes, gels, elastomers, and even rigid solids. Three types of dynamic measurements were carried out: (a) amplitude sweep; (b) frequency sweep; (c) parallel-plates dynamic mechanical thermal analysis.

TABLE III
The T_g, TGA, and DTG-Values for the BPPM-Acrylic Bone Cement Formulations

Formulation	T_g (°C)	T_{onset} (°C)	T_{peak} (°C)
BPPM-0	111.64	182.2	396
BPPM-10	89.95	248.3	401.4
BPPM-20	88.29	231.4	409.4

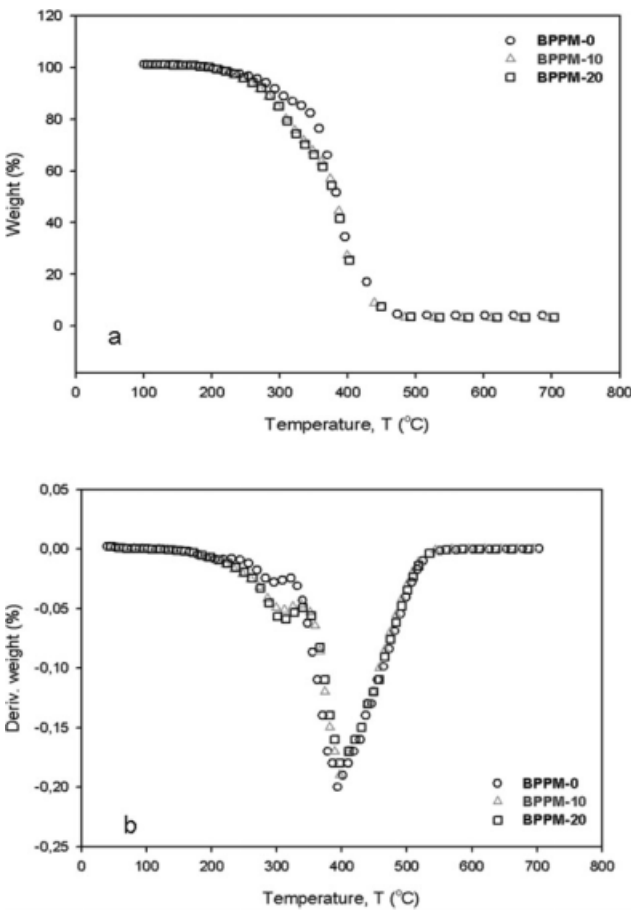

Figure 4 The TG (a) and DTG (b) thermograms for the BPPM-acrylic bone cement formulations.

TABLE IV
LVE Limits (Strain Amplitude, γ_L, and Shear Stress, τ_L), Together with G' and G''-Plateau Values within the LVE Range for the BPPM-Acrylic Bone Cement Formulations

Formulation	γ_L (%)	τ_L (Pa)	G' (Pa)	G'' (Pa)
BPPM-0	5	$2.48 \cdot 10^3$	$4.73 \cdot 10^4$	$1.67 \cdot 10^4$
BPPM-10	20	$1.26 \cdot 10^4$	$1.17 \cdot 10^5$	$5.12 \cdot 10^4$
BPPM-20	20	$2.00 \cdot 10^4$	$1.95 \cdot 10^5$	$8.52 \cdot 10^4$

The amplitude sweep is used to determine the linear-viscoelastic (LVE) range Table IV. Here, the oscillation frequency is kept constant ($\omega = 10\ s^{-1}$), while the oscillation amplitude (γ) is varied (between 0.01 and 100%). All the experiments were carried out at 160°C, above the glass transition temperature for all investigated acrylic bone cements. The limit of the LVE region indicates the maximum deformation tolerated by the sample before the internal superstructure is destroyed.

Figure 5 shows that at low oscillation amplitudes, within the LVE range, all three investigated bone cements exhibit G' and G''-constant plateau values.

The radiolucent cement (BPPM-0) presents a sharp decrease in G' and G'' beyond the upper limit of LVE region. The presence of BPPM units in the bone cement composition (samples BPPM-10 and BPPM-20) extends significantly the LVE range and generates higher G' and G''-values within the LVE region, suggesting more stable structures.

The frequency sweep is widely used as standard test in polymer rheology. In this test a sinusoidal strain with a constant amplitude ($\gamma = 5\%$) is applied and the

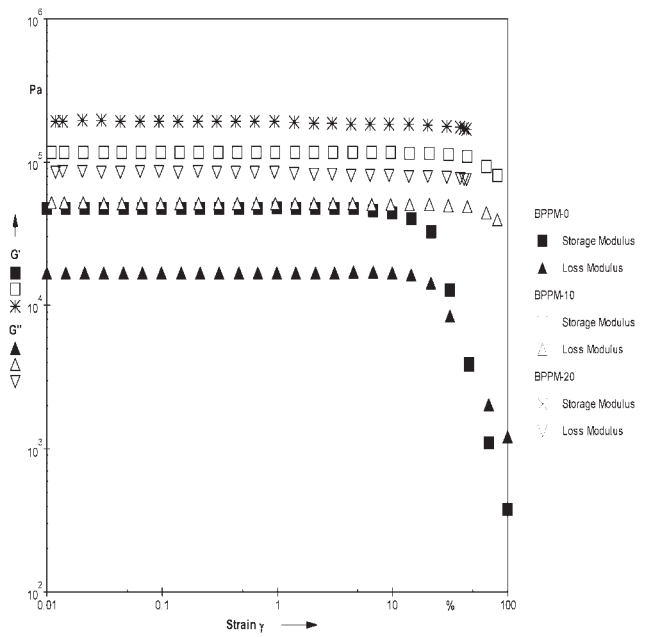

Figure 5 Amplitude sweep diagrams for: BPPM-0, BPPM-10, and BPPM-20.

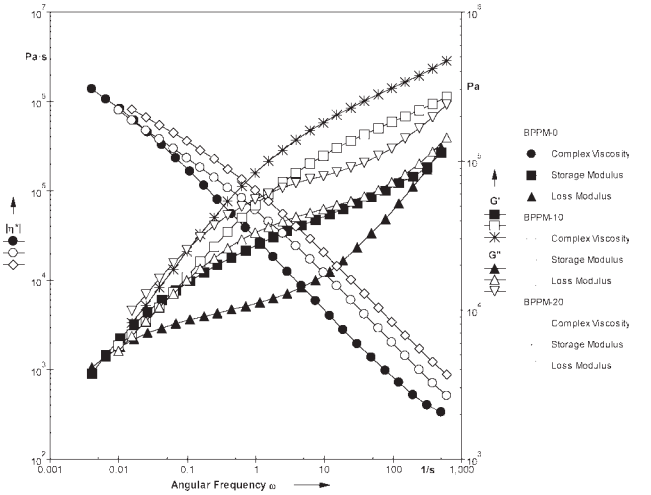

Figure 6 Frequency sweep diagrams for: BPPM-0, BPPM-10, and BPPM-20.

oscillation frequency is varied (between 10^{-2} and 10^3 s^{-1}). All measurements were carried out at 160°C.

Figure 6 presents the storage modulus G', the loss modulus G'' and the complex viscosity ($|\eta^*|$) for the same three bone cements as previously.

The radiolucent cement shows a typical behavior of polydisperse linear polymers[38]: the beginning of the viscous (terminal) region can be seen for frequencies below 10^{-2} s^{-1}, zone where G'' predominates due to the chains movements, i.e., reptation.

The so-called crossover point (the intersection point between G' and G''-curves), occurs at $5.9 \cdot 10^{-3}$ s^{-1} and $G' = G'' = 4.7$ kPa. Typically, the longest relaxation time can be determined as the inverse of the crossover frequency, $\omega_{crossover}$ (ω_{co}). For linear polymers, lower crossover frequencies indicate higher average molecular weight.

Above the ω_{co}, the rubbery (plateau) region appears, as a signature of polymer chain entanglements that act as temporary "network crosslinking points". Consequently, the elastic behavior of the sample dominates ($G' > G''$). BPPM-0 exhibits such behavior over five decades of frequency. Increasing more the oscillations frequency, the higher transition crossover region can also be detected for this sample where, due to high-frequency relaxation and dissipation mechanisms, the value of G'' rises much faster than G'. The second crossover point corresponds to $\omega = 374.5\ s^{-1}$ and $G' = G'' = 99{,}500$ Pa. This second crossover frequency normally can be related to the movements of the chain segments between two entanglements.

Considering the applicability of the Cox-Merz rule as valid for our systems, the rheological data were fitted with Carreau-Yasuda model,[19] using the rheometer software (Rheoplus):

TABLE V
Parameters of the Carreau-Yasuda Model

Formulation	η_0 (Pa s)	η_∞ (Pa s)	a	n	λ (s)	$G_{p,\exp}$ (Pa)	ω_p (s^{-1})
BPPM-0	$1.156 \cdot 10^6$	145.54	1.78	0.19	94.91	$3.5 \cdot 10^4$	3.4
BPPM-10	$9.892 \cdot 10^5$	$6.07 \cdot 10^{-5}$	0.772	0.26	42.17	$1.61 \cdot 10^5$	52.0
BPPM-20	$8.949 \cdot 10^5$	$1.05 \cdot 10^{-4}$	0.848	0.25	18.49	$2.64 \cdot 10^5$	47.2

$$|\eta^*| = \frac{\eta_0 - \eta_\infty}{\left[1 + (\lambda \cdot \omega)^a\right]^{\frac{1-n}{a}}} + \eta_\infty \quad (2)$$

where η_0 is the zero-shear viscosity, η_∞ is the infinite-shear viscosity. Regression parameters of the model: a, n and the λ (the characteristic relaxation time related to the onset of non-Newtonian or shear thinning behavior), were calculated using the rheometer software (Rheoplus). The rheological characteristics are listed in Table V, together with the characteristic plateau modulus ($G_{p,\exp} = G'(\omega)_{\tan\ \delta \rightarrow \text{minimum}}$) and its corresponding angular frequency (ω_p).

For comparing the rheological behavior of the BPPM-acrylic bone cements and the radiolucent one, we investigated the possibility of bringing all the experimental data [dynamic moduli and complex viscosity curves at 160°C in the same rheological conditions—Fig. 7(a,b)] together into single master curves, by means of appropriate shift factors. One has to keep in mind that the difference between the three investigated acrylic bone cements is the presence of some BPPM monomeric units on a number of polymer chains from the acrylic bone cements BPPM-10 and BPPM-20 (namely the copolymer chains formed via polymerization of the liquid monomer phase).

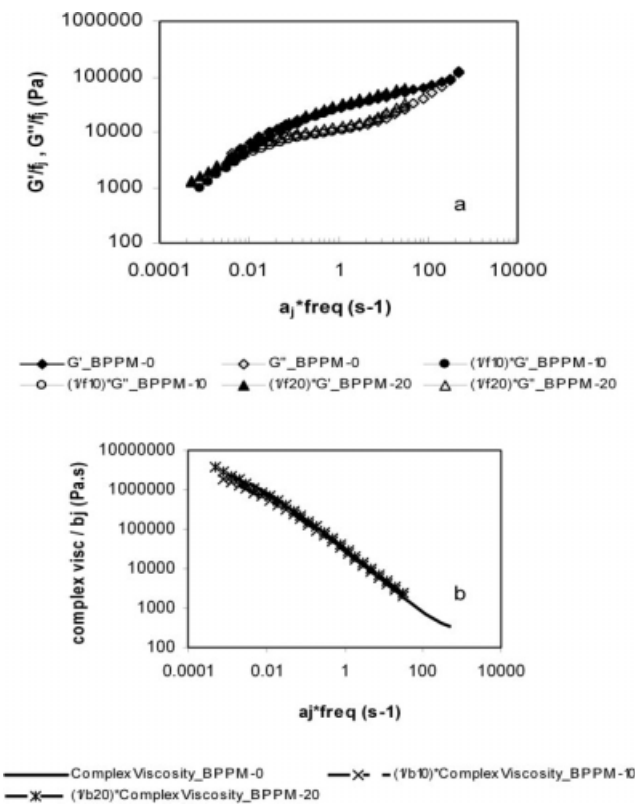

Figure 7 Master curves for BPPM-0, BPPM-10, and BPPM-20: (a) moduli curves; (b) complex viscosity curves.

The idea of master curves for the complex viscosity and dynamic moduli is based on the method of reduced variables. Three types of shift factors can be defined (Table VI): a_j, shift in angular frequency; f_j, shift in dynamic moduli (identical for G' and G''); and b_j, shift factor for the complex viscosity, where the subscript j indicates the corresponding acrylic bone cement. The shift factors were found by shifting the curves until they superpose to the reference ones (here the reference is BPPM-0). Additionally, it is found that the shift factors are interconnected by the following relation: $b_j = a_j \cdot f_j$.

The possibility of obtaining a master curve (Fig. 7) indicates that the two BPPM-modified cements exhibit comparable rheological behavior as the BPPM-0 cement, in the medium and high frequency range. Some differences exist at low frequencies, probably due to the BPPM later groups, which are modifying the reptation of the copolymers. The equivalent crossover points corresponds to 0.04 s^{-1} and 10.5 kPa for BPPM-10 and, respectively, 0.10 s^{-1} and 25.0 kPa for BPPM-20, indicating that the longest relaxation time diminishes when adding BPPM monomeric units.

Parallel-plates dynamic mechanical thermal analysis for the three samples was carried out in a temperature range between 30°C and 270°C, a heat rate of 5°C/min, at constant frequency of 1 Hz and constant strain amplitude $\gamma = 5\%$. Firstly, the

TABLE VI
Shift Factors for Building the Master Curves (Reference Curves: BPPM-0)

Shifted parameter	Shift factors	BPPM-0	BPPM-10	BPPM-20
Angular frequency, ω	a_j	1	0.05	0.05
Dynamic moduli, G', G''	f_j	1	8.50	4.25
Complex viscosity, $\lvert\eta^*\rvert$	b_j	1	0.425	0.21

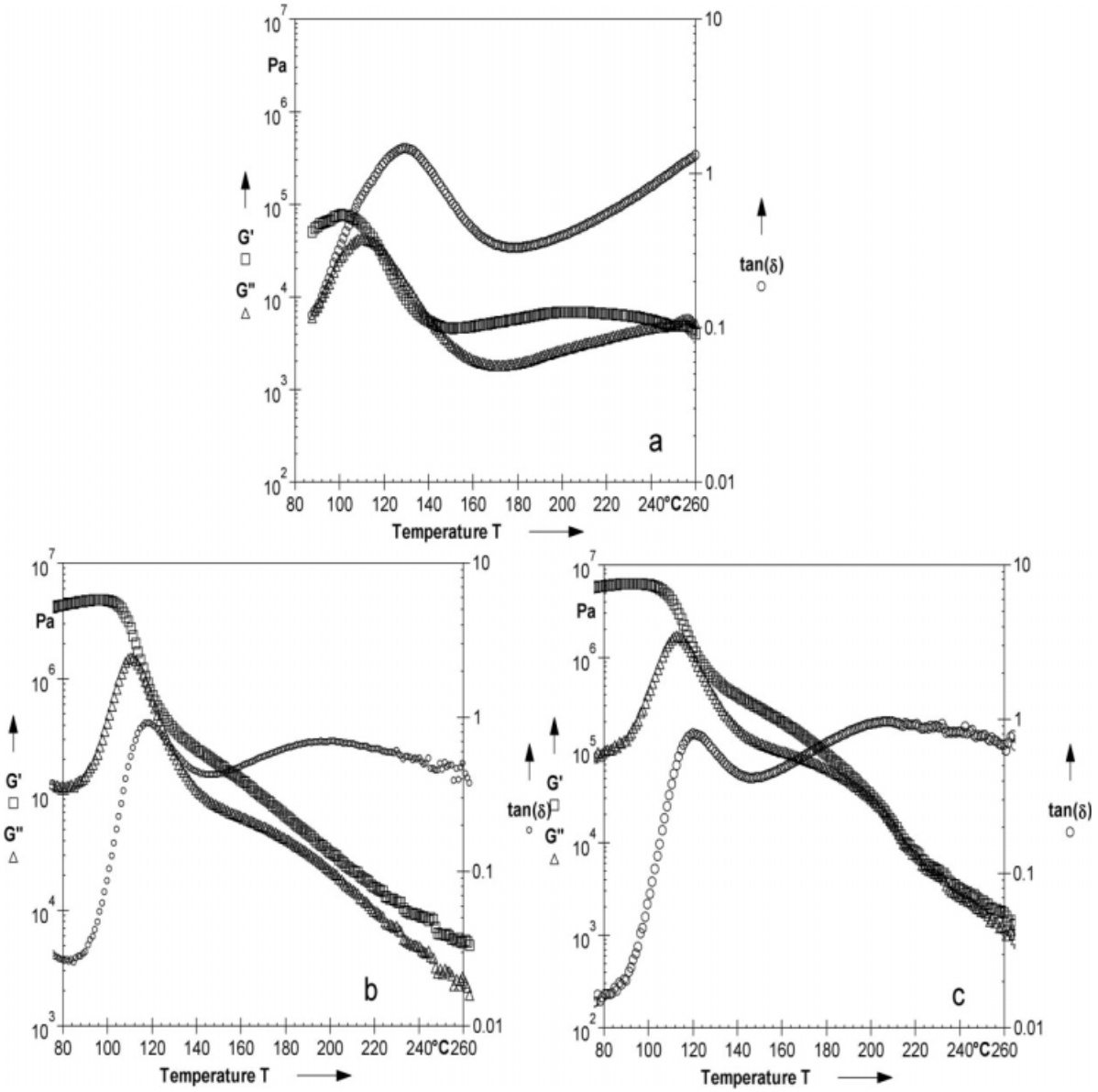

Figure 8 Parallel plates DMTA diagrams for: (a) BPPM-0; (b) BPPM-10; and (c) BPPM-20.

samples were melted at 200°C, under nitrogen atmosphere, to avoid thermal degradation, and then cooled down to 30°C. Figure 8 presents the temperature-dependence of the storage modulus G', the loss modulus G'' and the loss (or damping) factor, tan δ, where tan $\delta = G''/G'$.

This test allows measuring the transitions in polymers that present no chemical modification during the measurement. The focus is on softening and melting behavior and provides useful information on the type of material structure.

The drop in storage modulus and the peak in damping factor (tan δ) (Fig. 8) are due to the glass transition of the bone cements. Below glass transition temperature (T_g), the macromolecules are almost immobile and $G' > G''$. The polymer shows the consistency of a rigid and brittle solid. Increasing the temperature above T_g brings an increased mobility of the polymer chains. In the glass transition region, the material is in a soft-elastic, rubbery state. There are different methods to estimate T_g: as the maximum of G''-curve, or maximum of tan δ or the inflection point of the G'-curve. Each method provides slightly different results, so the observed T_g value should only be considered as estimative. Nevertheless, one can use the values from one given method to compare the three bone cements under investigation.

For the BPPM-0 cement, the T_g is either 109.6°C (as maximum of G''-curve), 116.9°C (as inflection point of G'-curve) or 129.9°C (maximum of tan δ), depending on the method. The softening range is

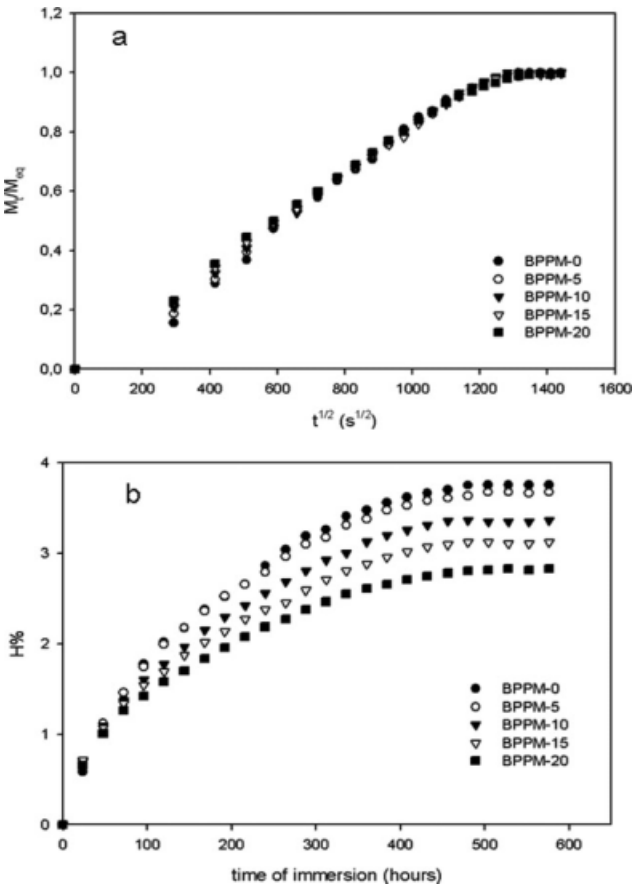

Figure 9 Water absorption for the BPPM-acrylic bone cement formulations: (a) water absorption versus $t^{1/2}$; (b) hydration degree as a function of immersion time.

situated between 116°C and 140.8°C. The softening process takes place gradually, and the temperature range is wider for a broad molar mass distribution. Finally, above 250.7°C, G'' becomes larger than G', indicating that the macromolecules move along each other, increasing the number of disentanglements. In this region, the radiolucent bone cement behaves as a viscoelastic liquid.

When adding 10% or 20% w/w of BPPM-comonomer in the liquid phase [Fig. 7(b,c)], some differences are observed. The behavior of samples is between that characteristic for linear and slightly crosslinked polymers. This could be an indication that some crosslinks are formed within the bone cement structures Literature is mentioning a network may develop during the curing process of acrylic bone cements when POB/tertiary ammine initiation system is used.[39,40] The estimated $(T_g)_{\text{maximum tan } \delta}$ is 120°C for BPPM-10 and 118°C for BPPM-20; one can recognize the same tendency as shown via DSC (see Table III), namely the presence of BPPM units inside the bone cement composition decreases its T_g.

Water absorption

Investigating the water absorption of the acrylic bone cements is very important for orthopedic applications, as the absorbed water influences the mechanical and biological properties of the bone cement.[12,15,32,41–44] Additionally, water absorption may induce hydrolysis of some (active) ingredients from the acrylic bone cement, which negatively influences the mechanical and biological properties. To a certain extent, water uptake may become beneficial for some medical applications, as for the dental filling materials, since the water swelling may compensate for polymerization shrinkage.[41–44]

The water absorption characteristics were determined by immersing cement disks (diameter 10 mm, thickness 3.5 mm) in distilled water, at room temperature, and continuously monitoring the evolution of the samples' weight. More specifically, the samples were weighed at different times until the water uptake was constant within 0.0005 g. Before each weighing (M_t), the samples were removed from water, dried on a filter paper and then rapidly weighed. The equilibrated samples were dried to constant weight (M_f) in a drying oven (60°C, under vacuum, 72 h).

The early stages of water uptake by acrylic bone cement are supposed to be diffusion-controlled and so, reasonably described by a reduced solution of Fick's Second Law of Diffusion (Stefan's approximation)[45]:

$$\frac{M_t}{M_{\text{eq}}} = 2\left(\frac{Dt}{\pi l^2}\right)^{1/2} \tag{3}$$

where M_t is the mass uptake at time t, M_{eq} is the equilibrium uptake, 2 L-thickness, D is the diffusion coefficient. This approximation is usually valid within the region where M_t/M_{eq} is linearly depending on $t^{1/2}$, typically for $M_t/M_{\text{eq}} < 0.5$. In these conditions, the diffusion coefficient D may be determined from the slope of the plot M_t/M_{eq} versus $t^{1/2}$. The experimental results for the different BPPM-acrylic bone cements are presented in Figure 9 and Table VII.

TABLE VII
Water Absorption Characteristics for the BPPM-Acrylic Bone Cement Formulations

Formulation	$D \cdot 10^8$ (cm^2/s)	n	H_{max} %	A%	E%
BPPM-0	1.80	0.46	3.75	4.82	1.24
BPPM-5	1.59	0.47	3.60	3.45	0.28
BPPM-10	1.58	0.48	3.35	3.24	0.25
BPPM-15	1.57	0.48	3.10	3.08	0.23
BPPM-20	1.56	0.46	2.80	3.04	0.20

Another way for quantifying the swelling kinetics of the acrylic bone cement formulations is based on the Frisch equation[46,47]:

$$\frac{M_t}{M_{\text{eq}}} = k \cdot t^n \quad (4)$$

where n indicates the type of process associated to water absorption.

The results from Figure 9(a) confirm that the new formulation of Fickian diffusion can be assumed for all acrylic bone cements, regardless the BPPM content, if considering the linear dependence obtained up to $M_t/M_{\text{eq}} = 0.8$. The corresponding diffusion coefficients vary in the range $1.56–1.8 \cdot 10^{-8}$ cm^2/s (Table VII). The decrease of the diffusion coefficient values when increasing the BPPM content in the acrylic bone cements may be explained once again by the slight crosslinking process due to the chain transfer capacity of the bromine-containing comonomer.

If expressing now the M_t/M_{eq} as a function of time, a power law time-dependence is obtain [as described in eq. (4)], and allow double-checking the type of mechanism assumed for the water uptaking, via the n values of the acrylic bone cements. The calculated n values range between 0.46 and 0.48 (Table VII), which points out that the water absorption does correspond to Fickian diffusion, for all the acrylic bone cements presented in this study.[48,49]

It is also worthwhile to determine the hydration degree (H%), water absorption (A%) and the percentage of elution (E%) for each of the experimental acrylic bone cement formulations, as following[32,47,50]:

$$H\% = \frac{M_t - M_0}{M_0} \cdot 100 \quad (5)$$

$$A\% = \frac{M_{eq} - M_f}{M_0} \cdot 100 \quad (6)$$

$$E\% = \frac{M_0 - M_f}{M_0} \cdot 100 \quad (7)$$

where M_0 is the initial weight of the specimen and M_f is the weight of the sample after testing.

One can see that the presence of the new synthesized BPPM comonomer in the acrylic bone cement formulations, has a positive effect on the magnitude of the water absorption: the maximum degree of hydration decreases linearly with increasing the BPPM content. Furthermore, all the BPPM-modified acrylic bone cements exhibit a lower elution (weight loss) than the radiolucent acrylic bone cement (see Table VII). One possible explanation is that the BPPM comonomer may induce a slight crosslinking during curing of the new cement formulations. This idea is also supported by the fact that all BPPM-cements are insoluble in ordinary solvents.

Density, polymerization shrinkage, porosity

The polymerization shrinkage and porosity of the BPPM-acrylic bone cements were estimated from experimental and theoretical density values. Cement shrinkage associated to the setting reaction comes with the transformation of a viscous material into hardened one, which generates an increase in density, and a volume decrease.[51] Quantitatively, the polymerization shrinkage (Sh) was determined as following[42]:

$$\%\text{Sh} = \frac{\text{density of polymer} - \text{density of monomer}}{\text{density of polymer}} \cdot 100 \quad (8)$$

The experimental shrinkage (Sh_{exp}) was determined via density measurements (experimental, i.e., apparent density, ρ_{exp}), while for the theoretical shrinkage (Sh_{theor}) the following relation was considered[21,42,52]:

$$\frac{\Delta V}{V}(\%) = 22.5 \cdot DC_{\text{mix}} \cdot \frac{\sum_i (f_i \cdot x_i)}{\sum_i (M_{mi} \cdot x_i)} \cdot \rho_{\text{mix}} \cdot 100 \quad (9)$$

where 22.5 is the volume change per mole of methacrylate groups (C=C) in MMA (cm^3/mol) when MMA is polymerized.[53,54] $DC_{\max}$ is the fractional degree of conversion, f_i is the functionality of monomer (i), x_i is the mole fraction of monomer (i), M_{mi} is the molecular mass of monomer (i), and ρ_{mix} is the density of the monomer mixture.

$$\%\text{Sh}_{\text{exp}} = \frac{\rho_{\text{exp}} - \rho_{\text{mix}}}{\rho_{\text{exp}}} \cdot 100 \quad (10)$$

$$\%\text{Sh}_{\text{theor}} = \frac{\rho_{\text{theor}} - \rho_{\text{mix}}}{\rho_{\text{theor}}} \cdot 100 \quad (11)$$

Maximum density (ρ_{theor}) is defined as the density of the bone cement completely free of pores and voids.[20] The results are summarized in Table VIII.

The analysis of these results shows first that both theoretical density (ρ_{theor}) and apparent density (ρ_{exp}) increase with the addition and subsequent increase of the ratio of bromine-containing comonomer in acrylic bone cement compositions. This increase is explained by the higher density of the BPPM-comonomer ($\rho_{\text{BPPM}} = 1.324$ g/cm^3) versus MMA ($\rho_{\text{MMA}} = 0.936$ g/cm^3).

Partially replacing MMA monomer with BPPM-comonomer in the liquid phase of the composition of acrylic bone cements reduces polymerization shrinkage (Table VIII). The decrease is more

TABLE VIII
Density, Polymerization Shrinkage, Porosity, and Water Contact Angle for the BPPM-Acrylic Bone Cement Formulations

Formulation	ρ_{theor} (g/cm^3)	ρ_{exp} (g/cm^3)	% Sh_{th}	% Sh_{exp}	% P	Contact angle
BPPM-0	1.129	1.094	5.70	4.80	3.15	74
BPPM-5	1.132	1.093	5.58	4.58	3.50	60
BPPM-10	1.136	1.099	5.46	4.51	3.31	61
BPPM-15	1.140	1.104	5.34	4.43	3.16	63
BPPM-20	1.145	1.110	5.22	4.33	3.06	65

significant when increasing the BPPM content in acrylic bone cements. This may be explained by the higher molecular weight of the BPPM-comonomer (M_{BPPM} = 266 g/mol) as compared with MMA (M_{MMA} = 100 g/mol). For a given gravimetric content of BPPM in acrylic cements composition, as its molecular weigh is higher, the number of moles is smaller than that of MMA, which means that the polymerization shrinkage is reduced, too.

Besides, experimental shrinkage values are lower than the theoretical ones, because of the presence of pores in the structure of the cured cements.

Another factor directly related to density and polymer shrinkage is the porosity of the sample, since cements with reduced porosity contract more during setting.[55] Porosity is always present in the cement structure as a consequence of the manual mixing of the powder and liquid components in air.[55–57]

Determination of polymer density gives values of the average percentage of porosity (%P) from the following expression[55,57]:

$$\%P = \left(1 - \left(\frac{\rho_{exp}}{\rho_{theor}}\right)\right) \cdot 100 \qquad (12)$$

The results presented in Table VIII show that the addition of bromine-containing comonomer in radiolucent acrylic cements composition induces only an insignificant increase of porosity. The slight increase of porosity may be explained by the reduction of the quantity of evaporated MMA during mixing, as a result of the reduced ratio of this monomer in liquid phase composition. All these results lead to the conclusion that the porosity of acrylic bone cements analyzed in this article is primarily due to the mixing method and, to a lower extent, to the composition of the liquid phase.

Water contact angle

As can be seen in Table VIII, the addition of bromine-containing comonomer in PMMA-cements formulations induces a decrease of the water contact angle. This means that the surface of acrylic bone cements becomes more hydrophilic with respect to the radiolucent PMMA-cement. However, this does not imply automatically an increase of the water absorption by the bulk BPPM-modified cements, as already presented in section Water absorption. The increased wettability of the new BPPM-cement formulations are expected to lead to a satisfactory cell adhesion since osteoblasts adhesion occurred preferentially onto moderately wettable surface and charged substrata.[30]

Compressive tests

In clinical service, the prosthesis is subjected to static or quasi-static direct compressive forces during certain activities, such as the one-legged stance. The cement mantle has been imagined as a compressive wedge between the femoral stem and the bone, while acting as shock absorber between the implant and bone.[29] As a consequence, the static compressive properties of the acrylic bone cement are very important.

Figure 10 shows the experimental results on compressive strength of BPPM-modified acrylic bone cements and the comparison with the radiolucent (pure) PMMA-cement. As can be seen, all acrylic bone cements fulfill the minimum compressive strength (70 MPa) required in ASTM Standard.[6] As a positive point, the partial replacement of MMA from the cement liquid phase with increasing amounts of

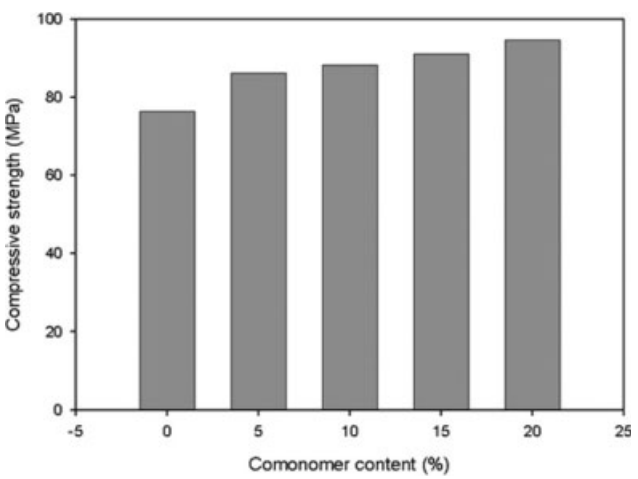

Figure 10 Compressive strength for the BPPM-acrylic bone cement formulations.

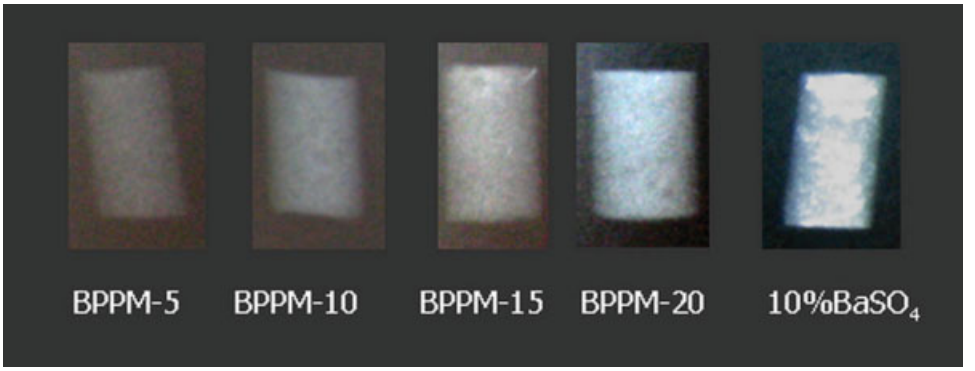

Figure 11 Radiographs for the BPPM-acrylic bone cement formulations and comparison with an acrylic bone cement containing 10% of $BaSO_4$. [Color figure can be viewed in the online issue, which is available at www.interscience.wiley.com]

bromine-containing comonomer increases the compression strength, which meanwhile remains comparable to the one of commercial acrylic bone cements.[21,24]

Radiopacity

All the new BPPM-acrylic bone cements are radiopaque, as shown in Figure 11, where a comparison with an equivalent acrylic bone cements containing 10% $BaSO_4$ is also proposed. As expected, the radiopacity degree does increase when increasing the amount of bromine-containing comonomer in the initial liquid phase of the acrylic cements.

CONCLUSIONS

A new bromine-containing acrylic monomer is proposed for obtaining radiopaque acrylic bone cements, the 2-(2-bromopropionyloxy) propyl methacrylate (BPPM), which was synthesized and characterized by ^{1}H NMR and ^{13}C NMR. Four experimental formulations of acrylic bone cements were realized, by partially replacing the MMA from the classical liquid monomer phase with 5–20% w/w of BPPM. It was established that the BPPM monomer in the initial liquid monomer phase does confer radiopacity to the acrylic bone cements. Furthermore, the presence of BPPM units in the acrylic bone cement composition improves the curing parameters, flexibility, thermal stability, polymerization shrinkage, and compression strength of the bone cements, without changing their water uptake, porosity, or contact angle.

References

1. Di Maio, F. R. Orthopaedics 2002, 25, 1399.
2. Kuhn, K. D. Bone Cements: Up-to-Date Comparison of Physical and Chemical Properties of Chemical Materials; Springer: Berlin, Germany, 2000.
3. Neuman, L.; Freund, K. G.; Sorensen, K. H. J. Bone Joint Surg B 1994, 76, 245.
4. Deb, S.; Vazquez, B. Biomaterials 2001, 22, 2177.
5. Demian, H. W.; Dermott, K. Biomaterials 1998, 19, 1607.
6. *** ASTM. Specification F 451–95. Standard specification for acrylic bone cement. Annu book of ASTM Standards, vol. 13.01: Medical Devices: Emergency Medical Services. Philadelphia: American Society for Testing Materials, 1996.
7. Ginebra, M. P.; San Roman, J.; Vazquez, B.; Planell, J. A. Biomaterials 2002, 23, 1873.
8. Artola, A.; Gurruchaga, M.; Vasquez, B.; San Roman, J.; Goni, I. Biomaterials 2003, 24, 4071.
9. Lewis, G. J Biomed Mater Res Part B: Appl Biomater 1997, 38, 155.
10. Manero, J. M.; Ginebra, M. P.; Gil, F. J.; Delgado, J. A.; Morejon, L.; Artola, A.; Gurruchaga, M.; Goni, I. J Eng Med 2004, 218, 3.
11. Molino, L. N.; Topoleski, L. D. T. J Biomed Mater Res 1996, 31, 131.
12. Lewis, G.; van Hooy-Corstjens, C. S.; Bhattaram, A.; Koole, L. H. J Biomed Mater Res Part B: Appl Biomat 2005, 73, 77.
13. Jayakrishnan, A.; Chithambara Thanoo, B. J. Appl Polym Sci 1992, 44, 743.
14. Davy, K. W. M.; Anseu, M. R.; Odlyha, M.; Foster, C. M. Polym Int 1997, 43, 142.
15. Vazquez, B.; Ginebra, M. P.; Gil, F. J.; Planell, J. A.; Lopez Brava, A.; San Roman, J. Biomaterials 1999, 20, 2047.
16. Aldenhoff, Y. B. J.; Kruft, M.-A. B.; Pijpers, A. P.; van der Veen, F. H.; Bulstra, S. K.; Kuijer, R.; Koole, L. H. Biomaterials 2002, 23, 881.
17. Benzina, A.; Kruft, M.-A. B.; Bar, F.; van der Veen, F. H.; Bastiansen, C. W. M.; Heijen, V.; Reuntelingsperger, C. Biomaterials 1994, 15, 1122.
18. Ichim, I. C.; Rusu, M. C.; Rusu, M.; Popa, M.; Delaite, C.; Riess, G. e-Polymer 2007, 066.
19. Mexger, T. G. The Handbook. The Users of Rotational and Oscillatory Rheometers, 2nd revised ed.; Vincentz Network: Hannover, Germany, 2006.
20. Coleman, M. M.; Graf, J. F.; Painter, P. C. Specific Interactions and the Miscibility of Polymer Blends; Technomic Publishing Company: USA, 1991.
21. Silikas, N.; Al-Kheraif, A.; Watts, D. C.; Biomaterials 2005, 26, 197.
22. Bettencourt, A.; Calado, A.; Amaral, J.; Alfaia, A.; Vale, F. M.; Monteiro, J.; Montemar, M. F.; Ferreira, M. G. S.; Castro, M. Int J Pharm 2004, 278, 181.
23. Lautershlager, E. P.; Moore, B. K.; Shoenfeld, C. M. J Biomed Mater Res Symp 1974, 5, 185.
24. Jefferis, C. D.; Lee, A. J. K.; Ling, R. S. M. J Bone Joint Surg A 1975, 37, 380.

25. Migliaresi, C.; Fambri, L.; Kolarik, J. Biomaterials 1994, 15, 875.
26. Huiskes, R. Acta Orthop Scand 1980, 185, (Suppl), 43.
27. Brauer, G. M.; Steinberger, D. R.; Stansburg, J. W. J. Biomed Mater Res 1986, 20, 839.
28. Pascual, B.; Goni, I.; Gurruchaga, M. J Biomed Mater Res Part B: Appl Biomater 1999, 48, 447.
29. Pascual, B.; Gurruchaga, M.; Ginebra, M. P.; Gil, F. J.; Planell, J. A.; Vasquez, B.; San Roman, J.; Goni, I. Biomaterials 1999, 20, 453.
30. Cervantes-Uc, J. M.; Vazquez-Torres, H.; Canich-Rodriguez, J. V.; Vasquez-Lasa, B.; San Roman, J. Biomaterials 2005, 26, 4063.
31. Vazquez, B.; Deb, S.; Banfield, W.; San Roman, J. J Biomed Mater Res Part B: Appl Biomater 2002, 63, 88.
32. Deb, S.; Braden, M.; Bonfield, W. Biomaterials 1995, 14, 1095.
33. Krause, W.R. In Encyclopedia of Medical Devices and Instrumentation, Webster, J. G.; Ed.; Wiley: New York, 1982; Vol. I.
34. Lewis, G. J Biomed Mater Res Part B: Appl Biomater 1997, 38, 155.
35. Saha, S. J Biomed Mater Res 1984, 18, 435.
36. Lewis, G. J Biomed Mater Res Part B: Appl Biomater B 2003, 66, 457.
37. El'Sheikh, H. F.; MacDonald, B. J.; Hashun, M. S. J. J Mater Process Technol 2003, 143, 249.
38. Barnes, H. A. Handbook of Elementary Rheology; Institute of Non-Newtonian Fluid Mechanics, University of Wales: UK, 2000.
39. Dnebosky, J.; Hynkova, V.; Hrabak, F. J Dent Res 1975, 54, 772.
40. Hrabak, F.; Hynkova, V.; Pivkova, H. Makromol Chem 1978, 179, 2593.
41. Ravell, P. A.; Braden, M.; Freeman, M. A. Biomaterials 1998, 19, 1579.
42. Deb, S.; Di Silvio, L.; Vasquez, B.; San Roman, J. J Biomed Mater Res Part B: Appl Biomater 1999, 48, 719.
43. Patel, M. P.; Braden, M.; Davy, K. M. W. Biomaterials 1987, 8, 53.
44. Bowen, R. L.; Rapson, J. E.; Dickson, G. J Dent Res 1982, 61, 654.
45. Crank, J. The Mathematics of Diffusion; Oxford University Press: London, 1956.
46. Allen, P. E. M.; Williams, D. R. G. Eur Polym Mater 1992, 28, 347.
47. Larraz, E.; Elvira, C.; San Roman, J. Biomacromolecules 2005, 6, 2058.
48. Ritger, P. L.; Peppas, N. A. J Control Release 1987, 5, 23.
49. Berriej, A. In Water in Polymers, 1st ed.; Crank, J.; Park, G. S., Eds.; Academic Press: New York, 1968.
50. Braden, M.; Clarke, R. L. Biomaterials 1984, 5, 369.
51. Pascual, B.; Gurruchaga, M.; Ginebra, M. P.; Gil, F. J.; Planell, J. A.; Goni, I. Biomaterials 1999, 20, 465.
52. Ward, I. M.; Hadley, D. W. An Introduction to Mathematical Properties of Solid Polymers; Wiley: Chichester, 1993.
53. Rose, E.; Lal, J.; Green, R. J Am Dent Assoc 1958, 56, 375.
54. Loshack, S.; Fox, T. G. J Am Chem Assoc 1953, 75, 544.
55. Hass, S. S.; Brauer, G. M.; Dickson, G. A. J Bone Joint Surg A 1975, 57, 380.
56. Molnar, E. J.; Grobor, R.; Sawyer, N. J Dent Res 1968, 47, 665.
57. Dunne, N. J.; Orr, J. F. Influence of mixing techniques on the physical properties of acrylic bone cement; 12th Conference of European Society of Biomechanics; Dublin, 2000, p 447.